



## Strengthening of RC Beams using Steel Plate-fiber Concrete Composite Jackets: Finite Element Simulation and Experimental Investigation

M. Shadmand, A. Hedayatnasab\*, O. Kohnehpooshi

Department of Civil Engineering, Sanandaj Branch, Islamic Azad University, Sanandaj, Iran

### PAPER INFO

#### Paper history:

Received 21 August 2021  
Received in revised form 29 September 2021  
Accepted 05 October 2021

#### Keywords:

Strengthening  
Simulation Method  
Concrete-steel Composite Jacket  
Load-Deflection Curves  
Crack Distribution  
Load Bearing Capacity

### ABSTRACT

In this research, steel plate-fiber concrete composite jackets (SPFCJ) was used to strengthen the RC beams. The accuracy of the analysis method was evaluated by modeling RC beams fabricated in the laboratory, and a good agreement was observed. Variables in the finite element method (FEM) analysis include the strength class of concrete used in the main beam (15, 20, and 25 MPa), the beam length (1.4 and 2.8 m), the type of jackets (RC jacket, SPFCJ, and CFRP sheet), and jacket thickness (40, 60 and 80 mm). SPFCJ is effective for all three concrete grades and increased the energy absorption capacity by 1.88, 2.07, and 2.25 times, respectively. The bearing capacity of the strengthened beam with 60 mm composite jackets increased by 79 and 20% more than the values corresponding to jackets with 40 and 80 mm thickness. The jacket thickness parameter significantly influences the response of strengthened beams with the proposed composite jackets. Depending on the dimensions and geometric characteristics of the beam, the appropriate thickness for the jacket should be considered, and increasing the thickness can not always improve the beam bearing capacity.

doi: 10.5829/ije.2022.35.01a.07

## 1. INTRODUCTION

Failure of reinforced concrete (RC) beams in the event of severe earthquakes may be due to insufficient steel reinforcement or non-compliance with new regulations [1-3]. Strengthening the beams and historical buildings in seismic design for RC structures is an important issue [4-8].

Researchers have considered the strengthening of RC beams in recent years [9-12]. Attar et al. [13] investigated the strengthened RC beams with self-compacting concrete (SCC) jackets containing fibers. The variables included the percentage of steel fibers (SFs), the effect of GFRP rebars, different ratios of longitudinal rebars, and the impact of shear rebars. The proposed concrete jackets improved the bearing capacity and the mid-span deflection of the beams by 44 and 25%, respectively [13]. Kim et al. [14] investigated the strengthened RC beams using modularized steel plates. The steel plates were

bolted to the beam surfaces. The dimensions of the plates were obtained using the finite element method (FEM). The proposed steel plates increased the bearing capacity by 7 times [14]. Rahimi et al. [15] investigated the effect of aramid fiber reinforcement polymer (AFRP) and glass fiber reinforcement polymer (GFRP) on the strengthened deep RC beams and compared their response with the performance of CFRP sheets. The number of FRP layers was 1, 2, and 3. Depending on the number of sheets, the addition of AFRP, CFRP, and GFRP sheets increased the bearing capacity by 65 to 94%, 87 to 130%, and 96 to 133%, respectively [15]. Artiningsih et al. [16] strengthened RC beams using the glass fiber jacketing system. Two different failure levels were considered for the beams. Depending on the failure level, the maximum load increased by about 52 to 115% [16].

Faez et al. [11] investigated the strengthened RC beams using concrete jackets containing aluminum oxide nanoparticles and silica fume. The results showed that

\*Corresponding Author Email: [Hedayatnasab\\_arastoo@yahoo.com](mailto:Hedayatnasab_arastoo@yahoo.com)  
(A. Hedayatnasab)

RC jackets containing aluminum nanoparticles, depending on the thickness jacket, the number of rebars used in the jackets, and the length of the beam span, have increased the flexural strength by 155 to 447% [11]. Mohsenzadeh et al. [12] investigated the strengthened RC beams using SCC jacket containing glass fiber and fibrous silica fume gel (FSFG). Concrete jackets containing glass fiber and FSCG, depending on the amount of glass fiber, have increased the energy absorption capacity of the beams by about 89 to 463%. Concrete jackets containing FSFG and glass fiber delay forming the concrete's first cracks and increase the energy absorption capacity [12].

On the other hand, steel fiber reinforced concrete (SFRC) has been considered due to many advantages [17-19]. According to previous studies, strengthened RC beams using steel plate-fiber concrete composite jackets (SPFCJ) were investigated in the present study. For this purpose, studies were performed in both laboratory and numerical sections. The experimental results of the proposed method were presented entirely by Shadmand et al. [20]. The results can be used in many RC buildings that have been damaged due to lack of adequate supervision, incorrect design, and executive errors. A new method has been introduced to strengthen RC beams. SFRC and steel jackets are used next to each other. In previous studies, the entire surrounding surfaces of the beams are strengthened using reinforcing elements; but in this research about 75% of the peripheral surfaces of the beams was retrofitted.

The mechanical properties of SFRC are evaluated by considering two variables: the amount of SFs (0, 0.5, 1, 1.5, and 2% of the concrete volume) and the category of concrete (40, 50, and 60 MPa). In the second part, the flexural load test of the beams was performed in the strengthening and without strengthening modes. The studied variables include the SFs (0, 1, and 2% of concrete volume) and the type of strengthening method (RC jacket, SPFCJ, CFRP sheet). In order to strengthen the beams with jackets, the dimensions of the beams were increased from the bottom and sides. At the end of laboratory studies, the beams' behavior was compared using load-displacement diagrams. After laboratory studies, several beams prepared in the laboratory were simulated using the FEM using ABAQUS software [21].

**2. THE STUDY PROCEDURE**

The flowchart of the study is presented in Figure 1. As can be seen, the present study was conducted in three sections: preliminary, laboratory, and numerical studies. The laboratory study was performed in two separate sections. In the first part, the mechanical properties of SFRC are evaluated by considering two variables: the amount of SFs (0, 0.5, 1, 1.5, and 2% of concrete volume)

and the strength category of concrete (40, 50, and 60 MPa). The experiments are presented in Table 1. The failure age of the samples was considered to be 28 days.

In the second part, the four-point flexural test of the beams was performed in the strengthened and non-strengthened modes. The studied variables include the amount of SFs (0, 1, and 2% of concrete volume) and the type of strengthening method (Table 2). Table 3 summarized the types of modes studied in the laboratory strengthening section.

Details of the proposed method are provided in the literature [20]. The loading device is shown in Figure 2.

**3. LABORATORY PROGRAM**

**3.1. Materials** The materials include coarse and fine aggregates, cement, water, superplasticizers, and

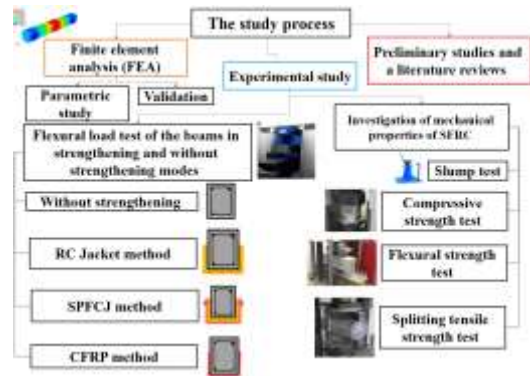


**Figure 1.** Flowchart of the study process

**TABLE 1.** Variables studied in laboratory study (Mechanical properties of SFRC)

<b>Category of concrete</b>	C40, C50, and C60
<b>The amount of SFs</b>	0, 0.5, 1, 1.5, and 2% volume of concrete
<b>Description:</b>	Slump, splitting tensile strength, compressive strength, and flexural strength tests were conducted.

**TABLE 2.** Variables studied in laboratory study (Laboratory strengthening) [20]

Name	Strengthening method	Steel fiber (%)
NR	-	-
J-F0		0
J-F1	RC jacket	1
J-F2		2
CJ-F0		0
CJ-F1	SPFCJ	1
CJ-F2		2
CFRP	CFRP	--

**TABLE 3.** The mixing scheme used in the study of the properties of SFRC

Name	Strength grade (MPa)	Cement (kg)	Gravel (kg/m <sup>3</sup> )	Sand (kg/m <sup>3</sup> )	Water (lit)	Steel fiber (%)	SP (%)
C40F0	40	400	839	801	180	0	1
C40F0.5	40	400	839	801	180	0.5	1
C40F1	40	400	839	801	180	1	1
C40F1.5	40	400	839	801	180	1.5	1
C40F2	40	400	839	801	180	2	1
C50F0	50	500	785	710	225	0	1
C50F0.5	50	500	785	710	225	0.5	1
C50F1	50	500	785	710	225	1	1
C50F1.5	50	500	785	710	225	1.5	1
C50F2	50	500	785	710	225	2	1
C60F0	60	600	678	672	270	0	1
C60F0.5	60	600	678	672	270	0.5	1
C60F1	60	600	678	672	270	1	1
C60F1.5	60	600	678	672	270	1.5	1
C60F2	60	600	678	672	270	2	1

C: Concrete grade (Strength) F: Steel fiber SP: Superplasticizer

SFs. Coarse and fine aggregates grading test is conducted. The apparent density of the sand in saturated state with dry surface is 2.6 ton/m<sup>3</sup>. The apparent density of gravel in saturated state with dry surface is 2.65 t/m<sup>3</sup>.

Portland cement type II was used. The density and specific surface area of cement were 3.16 g/cm<sup>3</sup> and 3350 cm<sup>2</sup>/g, respectively. The superplasticizer is liquid and its color is brown. Its density is 1.1 g/cm<sup>3</sup>. The steel fibers are simple with hooked ends. Detailed specifications of materials are provided in the literature [20].

**3. 2. Experimental Tests** Figure 3 shows the experiments. The fresh concrete properties were evaluated using the slump test following ASTM C143 [22]. The compressive strength test was performed following ASTM C39 [23]. The flexural strength of concrete was performed following ASTM C293 [24]. The splitting tensile strength test was conducted following ASTM C496 [25]. For this purpose, cylindrical specimens with dimensions of 15×30 cm were prepared and tested.

Geometric dimensions of the beams and steel reinforcement characteristics were selected based on laboratory facilities and studies in retrofitting the RC beams. The main beams' length, width, and height were considered as 1600, 150, and 200 mm, respectively (Figure 4) [20].

**3. 3. Mixing Design** The standard mixing design

method of ACI-211 [26] regulation is used. The mixing plan of concrete samples prepared in the technology section, main beams, and concrete jackets presented in Tables 3 and 4. During concreting, sand, gravel, cement, and water were mixed with a mixer for two minutes, and then the SFs, which were clean and free of any waste and

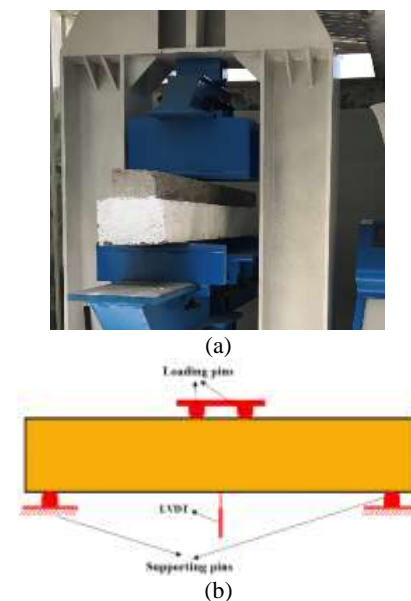


**Figure 2.** Four-point flexural test a: Loading frame b: LVDT, Supports, and the loading pins of the beams [18]



**Figure 3.** Experimental tests a: Slump test (b) Cubic specimens (c) Mixing concrete (d) Compressive strength (e) Splitting tensile strength f: Flexural strength

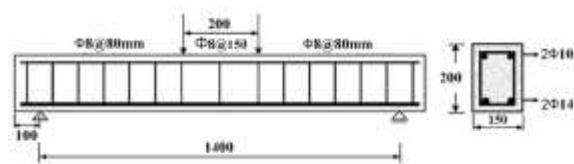


**Figure 4.** Geometric properties [20]

oil, were gradually poured into the mixer. After adding the fibers, the mixer was allowed to run for another three minutes until the fibers were spread throughout the concrete and the mixture was completely uniform.

**TABLE 4.** Mixing design used to make beams and jackets [18]

Member	Mix code	$\frac{W}{C}$	C (kg/m <sup>3</sup> )	G (kg/m <sup>3</sup> )	S (kg/m <sup>3</sup> )	F (%)	SP (%)
Original Beam	NR	0.45	350	955	885	-	-
RC Jacket	J-F0	0.45	500	785	710	0	1
	J-F1	0.45	500	785	710	1	1
	J-F2	0.45	500	785	710	2	1
	CJ-F0	0.45	500	785	710	0	1
	CJ-F1	0.45	500	785	710	1	1
	CJ-F2	0.45	500	785	710	2	1

W: Water C: Cement G: Gravel S: Sand F: Steel fiber SP: Superplasticizer

## 4. TEST RESULTS

**4. 1. Workibility and Mechanical Properties** The properties of fresh concrete were investigated using the slump test. According to ACI 211.1-91 [26-28], the allowable range slump is 25 to 100 mm for reinforced concrete beams. The slump values for 15 typical concrete samples are shown in Figure 5. The slump values of all 15 samples are within the allowable limits of the regulations. The increase in compressive strength under the influence of fibers can be explained by the fact that the presence of fibers delays the growth of fine cracks in concrete, which in turn increases the resistance and strain under maximum load (Table 5) [29-31]. The fibers prevent microcrack spread, leading to greater compressive strength. While at the macro scale, it increases energy absorption [32, 33].

It is observed that the addition of SFs to concrete samples, can increase the tensile strength of concrete samples from 1.5 to 50.1%.

Special attention is paid to the shape of the fibers used (hooked), which leads to an increase in their elongation resistance as a result of improving the matrix-fiber continuity [32-34]. Also, it is observed that the addition of SFs to ordinary concrete samples, depending on the

amount of fibers and concrete category, can increase the flexural strength of concrete samples from 3.1 to 50.1 %.

**4. 2. Results of Four-point Bending Test** The four-point bending test and crack distribution results are presented in the literature [20]. The crack distribution of the beams is illustrated in Figure 6. Load-deflection curves are presented in Figure 7. Also, crack load ( $P_{cr}$ ), yield load ( $P_y$ ), maximum load ( $P_u$ ), crack deflection ( $\Delta_{cr}$ ), yield deflection ( $\Delta_y$ ) and ultimate deflection ( $\Delta_u$ ), ductility, stiffness, and adsorption capacity, the energy absorption are presented in Table 6. Each of the parameters is stated in Figure 8.

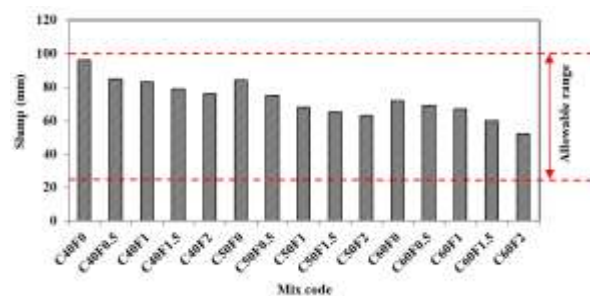


**Figure 5.** Slump values of samples in different mix proportions

**TABLE 5.** The test results (Mechanical properties)

Name	Compressive strength (MPa)	Variation (%)	Splitting tensile strength (MPa)	Variation (%)	Flexural strength (MPa)	Variation (%)
C40F0	36.9	-	3.12	-	4.21	-
C40F0.5	37	0.3	3.28	5.1	4.34	3.10
C40F1	37.1	0.5	3.89	24.7	4.5	6.90
C40F1.5	37.4	1.4	3.91	25.3	5.39	28
C40F2	37.6	1.9	3.98	27.6	6.32	50.10
C50F0	44.1	-	3.41	-	4.81	-
C50F0.5	44.2	0.3	3.9	14.4	5.1	6
C50F1	44.5	0.9	4.30	26.3	5.62	16.80
C50F1.5	45.1	2.3	4.80	40.8	5.93	23.30
C50F2	45.3	2.7	5.10	49.6	7.10	47.60
C60F0	52.1	-	3.85	-	5.10	-
C60F0.5	52.6	1	4.23	9.9	5.81	13.90
C60F1	53.2	2.1	4.61	19.8	5.91	15.90
C60F1.5	53.8	3.3	5.20	35	6.15	20.60
C60F2	54.1	3.8	5.80	50.1	6.41	45.30



NR



J-F0



J-F1



J-F2



CJ-F0



CJ-F1



CJ-F2



CFRP

**Figure 6.** Crack distribution [18]

**4. 3. Comparative Study with Other Studies** To compare the performance of the method proposed in this section, a comparative study of this method with similar studies has been conducted.

In the study of Ying et al. [35], the method of steel plates and rebar planting was used to strengthen RC beams, and the highest rate of increase in bearing capacity was reported to be 1.47. In the study of Abdulla [36], jackets containing cement mortars reinforced with glass fibers and carbon fibers were used to strengthen the beams, and the bearing capacity of the beams was increased by 1.33 times in the maximum case. Abdullah et al. [37] investigated the strengthening beams using CFRP rebars buried in the surface. The maximum increase in bearing capacity compared to the reference samples was 1.59 [37].

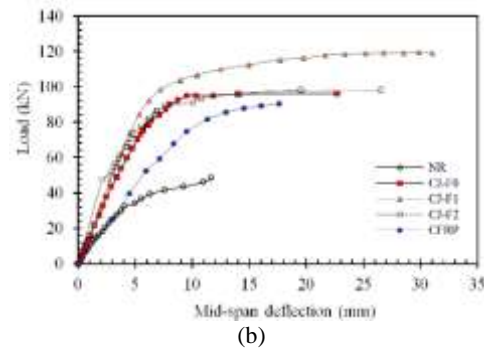
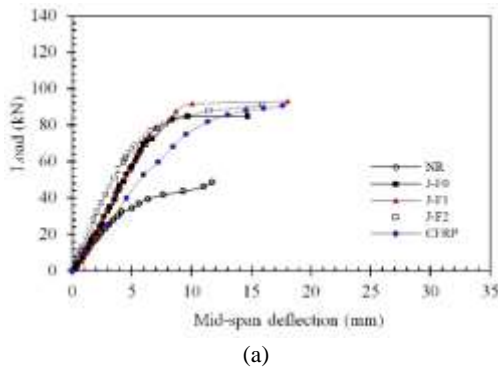


Figure 7. Load-deflection a: RC jackets b: SPFCJ [18]

TABLE 6. Crack, yield, and maximum point values

Code	Load (kN)			Mid-Span deflection (mm)			Ductility index	Stiffness (N/mm)	3
	Crack point	Yield point	Max. point	Crack point	Yield point	Max. point			
NR	4.1	34.2	52	0.5	5	11.7	2.34	8228.6	382
J-F0	7.2	66.3	85	1	5.7	14.7	2.58	8605.7	916
J-F1	9.3	68.9	93	1.30	6.16	17.9	2.69	922.2	1097
J-F2	9.0	68.7	91	1.20	5.9	15.9	2.91	8948.6	1266
CJ-F0	11.1	87.2	96.1	1.80	7.7	22.7	2.95	185085.7	1822
CJ-F1	12.9	101	119	2.4	8.95	31.8	3.55	16457.1	3119
CJ-F2	13.6	89.3	98.1	2.1	7.73	26.6	3.44	16525.7	2259
CFRP	5.1	62.3	90.8	0.89	7.3	17.5	2.40	8537.1	1074

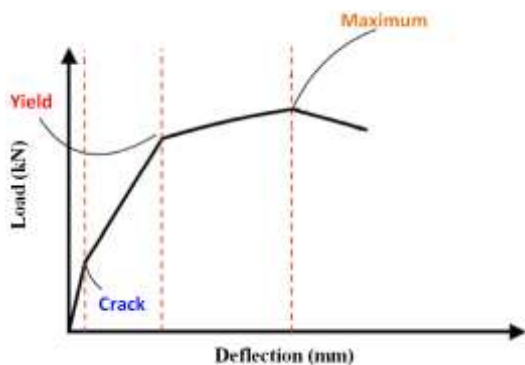


Figure 8. Hypothetical load-displacement diagram

Faez et al. [11] investigated the reinforcement of reinforced concrete beams using concrete jackets containing aluminum oxide nanoparticles. In this study, the highest rate of increase in bearing capacity was 2.75. Nanda and Bahra [38] used the method of gluing GFRP sheets in beam reinforcement. The results showed that this method could increase the bearing capacity by 1.34 times. Yu et al. [39] investigated the strengthening of severely damaged concrete beams using CFRP sheets. They showed that installing CFRP sheets can increase the

maximum beam load by about 2.13 times. Zhang et al. [40] used concrete layers to strengthening RC beams and showed that this method could improve the bearing capacity by about 2.2 times. The present study results also showed that using SPFCJ containing SFs can increase the bearing capacity of beams by about 2.28 times.

### 5. FINITE ELEMENT ANALYSIS

The high cost of experimental experiments in civil engineering has necessitated the evaluation of software simulation methods. Due to the wide range of parameters involved in beam strengthening, decisions about design strategies and components are virtually impossible without simulation tools. In order to use the simulation tools correctly in the design and evaluation process, it is necessary to check their validity through scientific methods because the validity and accuracy of such devices are affected by various factors and require appropriate software depending on the type of parameters and data. In this research, the validity of simulation software (ABAQUS) has been investigated by experimental method.

This section describes the simulation method used. The simulated components include the main beam, the main beam longitudinal rebars, the transverse rebars in the main beam, the concrete jacket, steel reinforcement of the jacket steel plate for SPFCJs, the CFRP sheets and the distributed steel plates. The behavior of these models was defined in the Part section of the software. The main beams, concrete jacket, and load-bearing steel plates were determined using the solid element. Solid elements have a special place in terms of being the most used among the types of elements.

Longitudinal rebars of the main beam, transverse rebars in the main beam, and steel reinforcement rebars of the jackets were defined using the Wire element. CFRP sheets and steel plates were defined for use in SPFCJ using the shell element. Concrete, steel, and CFRP sheets are among the materials defined in the modeling of the beams under study in different states. The properties of these materials are applied in the property section. Poisson's coefficient of concrete was considered 0.2. Also, the resistance classes of the main beams were considered C15, C20, and C25, respectively. Compressive and tensile strengths of the mentioned categories were performed by performing compressive and tensile strength tests. Table 7 lists the specifications for these concretes.

Also, from the mixing designs considered for reinforced concrete with SFs, a design was selected in which one percent of SFs was used. This choice is because this mixing design had better results in compressive, tensile, and flexural strengths than other designs. The compressive strength and tensile strength of this design were 37.1 MPa and 3.89 MPa, respectively. Steel rebars are ribbed and A3. Figure 9 shows the stress-strain diagram of the rebars.

The concrete structure was defined using the concrete damage plasticity (CDP). This model can show the nonlinear behavior and failure characteristics of brittle materials such as concrete. The CDP model in ABAQUS software is based on the model presented by Lulliner et al. [41]. The main priority of the damaged concrete plastic model is to provide the ability to analyze

**TABLE 7.** Specifications of concretes used in main beams and proposed jackets

Member	Concrete grade	Steel fiber (%)	Compressive strength (MPa)	Splitting tensile strength (MPa)
Main beam	C15	0	15.6	1.58
	C20	0	20.5	2.1
	C25	0	27.3	2.26
RC jacket	C40	1	37.1	3.89

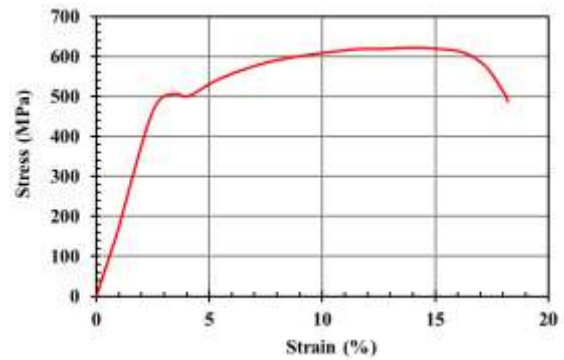


**Figure 9.** Stress-strain diagram of simulated rebars

concrete structures under cyclic or dynamic loads. The behavior of concrete under low confinement pressure is generally brittle, which means that the main mechanism of failure is to create cracks in tension and crushing in pressure. If the confinement pressure is large enough to prevent cracks from spreading, then the brittle behavior of the concrete becomes ductile. This model assumes that the two main factors in concrete failure are cracking due to tension and crushing under pressure [42-44]. This model assumes that the strain rate is obtained from the sum of the elastic and plastic strain rates. In general, it can be said that the inelastic response of models in ABAQUS is divided into two separate parts: elastic response with reversible and inelastic with irreversible (permanent). This assumption is the primary basis of the following relation:

$$\varepsilon = \varepsilon^{el} + \varepsilon^{pl} \quad (1)$$

The concrete structure was defined using the CDP model. This model can show the nonlinear behavior and failure characteristics of brittle materials such as concrete. The strain rate of the elastic and plastic part and the strain rate of the plastic part. Two stiffness variables control changes in the yield procedure (or failure procedure)  $\varepsilon_t^{pl}$  and  $\varepsilon_c^{pl}$  which depend on the failure mechanism under tensile and compressive loads, respectively.

Figures 10 and 11 show concrete's tensile stress and axial response defined under the plastic damage parameter. It is assumed that under uniaxial stress; The stress-strain response of concrete is linear up to the yield stress phase  $\sigma_0^t$  (Figure 10), the flow stress occurs at the same time as the formation of fine cracks in concrete materials. After yield tension; The response to softening stress and the appearance of fine cracks is macroscopically visible and causes strain accumulation (permanent deformation) in concrete materials. On the other hand, under uniaxial pressure, it is assumed that the response is linear up to the initial yield stress stage (Figure 11). After initial yield, the strain stress response is typically defined by the stress hardening behavior

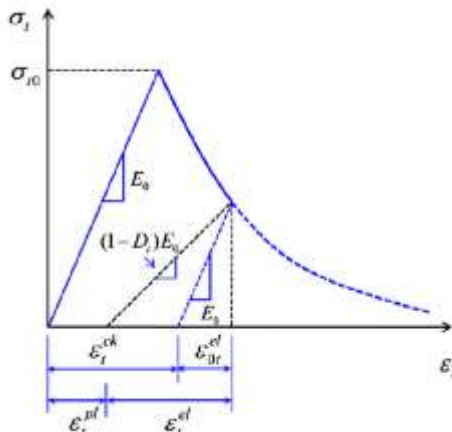


**Figure 10.** Definition of tensile properties of concrete in CDP model [21]

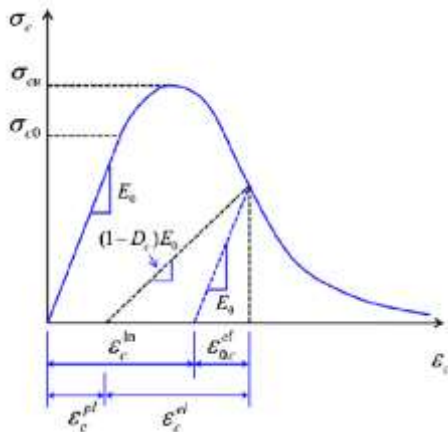


**Figure 11.** Definition of compressive properties of concrete in CDP model [21]

followed by strain-softening until the ultimate stress stage  $\sigma_{cu}$ . These hypotheses, despite their simplicity, cover the main capabilities of the concrete response. In this case, the strain stress relationship can be written according to the scalar variable of concrete damage as Equations (3) and (4) [21]:

$$\epsilon_t^{pl} = \epsilon_t^{ck} - \frac{d_t}{(1-d_t)} \frac{\sigma_t}{E_0} \tag{3}$$

$$\epsilon_c^{pl} = \epsilon_c^{in} - \frac{d_c}{(1-d_c)} \frac{\sigma_c}{E_0} \tag{4}$$

In this regard,  $E_0$  is the initial elastic modulus (undamaged concrete) which, after multiplication in the damage parameters  $(1-d_t)$  and  $(1-d_c)$  becomes the variable of concrete damage. In other words, if the concrete is loaded in this state, it will respond with a gentler slope than the initial state in the strain stress curve. This is due

to the damage done to it in the previous loading. In practice, the hardness of the current damaged condition is less than the hardness of the original undamaged state of the concrete sample. The value of the damage variables  $d_t$  and  $d_c$  can range from zero, which represents no damage; If we ignore the elastic part with linear curves, in this case, the plastic strain curve of plastic stress is obtained. This means that the values of elastic stress and strain must be removed from the program input values. It is worth mentioning that the program can find the yield strain by dividing the yield stress by the elastic modulus of concrete and, therefore, practically the elastic part of the strain stress curve, which is linear. It is necessary to define the dilation angle values, eccentricity, K coefficient, and Poisson's coefficient. The dilation angle expresses the relationship between volumetric strain and shear strain. The expansion angle is considered to be greater than the internal friction angle of the concrete. The eccentricity potential of plastic is a small positive number equal to the tensile strength ratio to compressive strength of concrete. K is the coefficient that is considered 0.667 for concrete by default. The viscosity parameter is a parameter that is regarded as 0.00 by default. Table 8 presents the values of the parameters required to use the "concrete with damaged plasticity" model.

The thickness of CFRP fibers used is equal to 1 mm, and its unit mass of surface area is similar to 1536 N/m<sup>2</sup>, and its Poisson coefficient is equal to 0.25, and its modulus of elasticity is equal to  $2.4 \times 10^5$  MPa. Defining interactions between different members in ABAQUS simulation is one of the steps that must be done with great precision. The Embedded region was used to determine the interaction between steel rebars and concrete. Using the interaction module and clicking on constraint, the constraints were selected, and first, the buried area (reinforcements) was established, then the concrete area was selected for the host.

Definition of interaction between RC jackets and main beam, Definition of interaction between composite steel jackets and main beam, the interaction between steel plates and concrete jacket, and interaction between FRP and the main beam was done using tie element. The advantage of using the tie constraint is that it facilitates

**TABLE 8.** Specifications of concrete materials introduced to the software [45]

Parameter	
Dilation angle	°36
Eccentricity parameter	0.1
K	0.667
Viscosity	0
Poisson coefficient	0.2

the meshwork, and two pieces can have completely different mesh. At the point of contact, the two pieces should have the same mesh; depending on the complexity of the model, geometry may be a little difficult.

At ABAQUS, there are two different types of meshing methodologies called top-down and bottom-up. Of course, sometimes, the two meshing methodologies refer to automatic meshing and manual meshing, respectively, which refers to using and implementing each of these methods. Four different meshing techniques can be used Structured, sweep, accessible and Bottom-up. The first three techniques use the top-down methodology, and the last technique uses the bottom-up method to generate the mesh. It should be noted that not every piece of geometry can be meshed using any of the above methods. This parameter is entirely qualitative and is limited only to compare the degree of simplicity in meshing two different pieces. The Meshability of a piece can always be increased by partitioning it into a mesh module and dividing it into simpler sections, reducing the complexity. The structured sweep technique was used. In this case, there is the most control over the elements. Figure 12 shows the types of simple patterns for meshing more complex parts.

The basis of the solution in finite element software is the meshing and division of the main model into a limited number (limited means a definite number and does not imply the limit on the number) of smaller components. But the main question is: how many of these small members are needed to have a reliable solution? This question does not have a unique answer, but a criterion must be set to reach a reasonable response in choosing the number of elements. One of the most important parameters in solving finite elements is discussing the time and cost of solving. This parameter directly depends on the number of elements created. If 100 elements are selected for networking a problem, it will take less time to solve the same problem than solving the same problem with 200 elements. The number of elements and the elements' geometry and appearance are effective parameters in the discussion of convergence. First, a reasonable number of elements must be used. One of the essential points in determining the initial number of elements is the discussion of geometry and meshing order.

The optimal mesh size in the studied beams was calculated using the trial and error method. Based on this, the mesh dimensions considered to be 35 mm. Figure 12 shows an example of modeling.

## 6. VALIDATION

One of the essential parts of software simulations is to check the accuracy of the simulation method used. Validation is the process of evaluating a simulation



**Figure 12.** A picture of the meshing of several models

method to check whether the software used is properly accurate or not. In the present study, four beams prepared in the laboratory were simulated using the modeling method. Their responses were compared with each other in the form of load-displacement diagrams. The names and specifications of the selected beams are presented in Table 9. Among the beams prepared in the laboratory, beams named NR, J-F1, CJ-F1, and CFRP were simulated. The NR beam is the same as the control beam or non-strengthened beam. CJ-F1 is a beam whose peripheral surfaces are reinforced with SPFCJ containing 1% SFs.

Figures 13a to 13c show the crack distribution and load-displacement diagrams of the finite element model and the laboratory sample of the NR beam. Crack, yield and maximum loads, and energy absorption capacity of the NR beam finite element model are 3.8, 34.9, and 44.3 kN and 378 kJ, respectively. Crack loads, yield, and maximum laboratory samples of NR beam were 4.1, 34.2, and 48.5 kN and 382 kJ, respectively.

**TABLE 9.** The variables studied in the present study

Beam name	Strengthening method	Fibers used in the jacket (%)
NR	Control beam (C20)	-
J-F1	RC Jacket	1
CJ-F1	Steel Plate-Fiber Concrete Composite Jackets	1
CFRP	CFRP	-

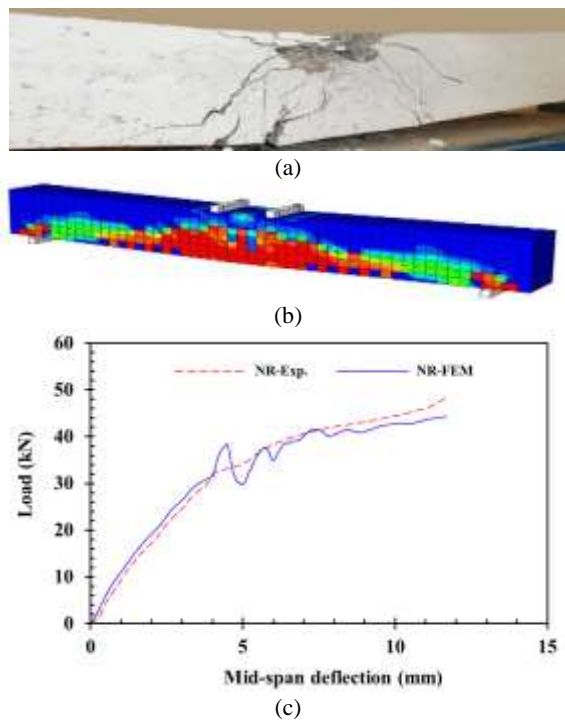


**Figure 13.** (a) Crack distribution in NR beam laboratory samples (b) Crack distribution in the finite element model of NR beam (c) Comparison of load-deflection diagrams of NR beam

Figures 14a to 14c show the crack distribution and load-displacement diagrams of the finite element model and the laboratory sample of the J-F1 beam. Crack, yield, maximum loads, and energy absorption capacity of the J-F1 finite element model are 9.6, 72.6 and 87.8 kN, and 1319 kJ. Crack loads, yield, and maximum laboratory sample of J-F1 beam are 9.3, 68.9, and 93 kN, and 1097 kJ, respectively.

Figures 15a to 15c show the crack distribution and load-displacement diagrams of the finite element model and the laboratory specimen of the CJ-F1 beam. Crack, yield and maximum loads, and energy absorption capacity of the CJ-F1 finite element beam model are 13.1, 99, and 121 kN and 2983 kJ, respectively. Crack loads, yield, and maximum laboratory samples of CJ-F1 beam are 12.9, 101, and 119 kN and 3119 kJ, respectively.

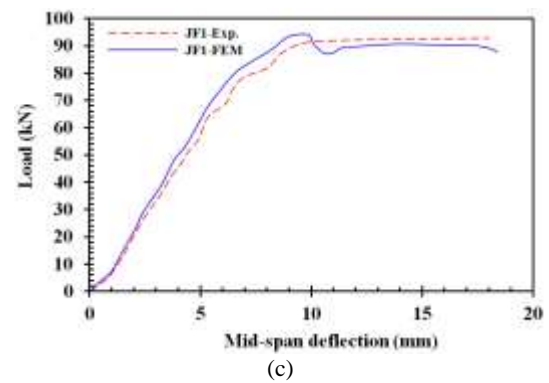
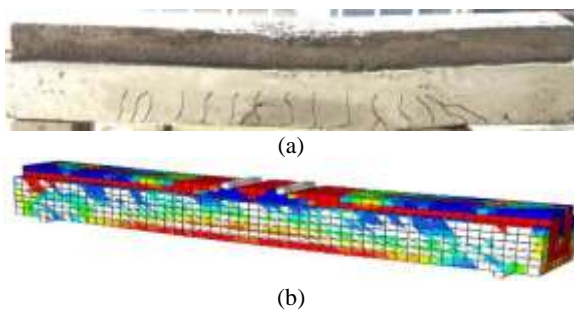


**Figure 14.** (a) Crack distribution in J-F1 beam laboratory samples b: Crack distribution in the finite element model of NR beam c: Comparison of load-deflection diagrams of J-F1 beam

Figures 16a to 16c show crack distribution and load-displacement diagrams of the finite element model and the laboratory sample of CFRP beams. Crack, yield and maximum loads, and energy absorption capacity of the CFRP finite element model are 5.4, 68.4, and 92.6 kN and 1145 kJ, respectively. Crack, yield, and maximum laboratory loads of CFRP beam are 5.1, 62.3, and 90.8 kN and 1074 kJ, respectively.

Table 10 shows the percentage of load differences related to laboratory samples and finite element models. In the NR beam, the difference of crack load is about 7.9%, the difference of yield load is about 2%, and the maximum load difference is about 8.6%.

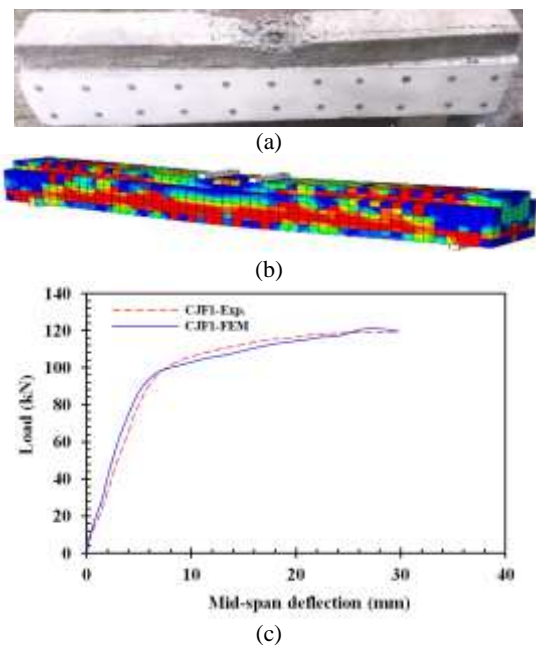


**Figure 15.** a: Crack distribution in CJ-F1 beam laboratory samples b: Crack distribution in the finite element model of CJ-F1 beam c: Comparison of load-deflection diagrams of CJ-F1 beam

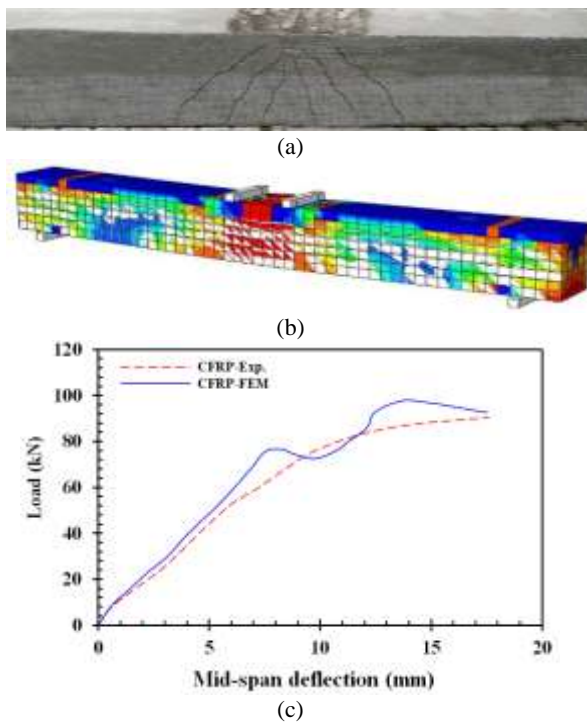


**Figure 16.** (a) Crack distribution in CFRP beam laboratory samples (b) Crack distribution in the finite element model of CFRP beam (c) Comparison of load-deflection diagrams of CFRP beam

In the J-F1 beam, the difference between crack load is about 1.3 percent, yield load difference is about 5.1 percent, and maximum load difference is about 5.9 percent. In the CJ-F1 beam, the difference between crack load is about 1.5 percent, yield load difference is about 2 percent, and maximum load difference is about 1.7 percent. In CFRP beam, the difference of crack load is about 5.6%, the difference of yield load is about 8.9%, and the maximum load difference is about 1.9%. According to the obtained values, it can be stated that the method used in simulating reinforced beams with concrete jacket, SPFCJ, and CFRP techniques has good accuracy, and this method can have an acceptable prediction.

## 7. FEA RESULTS

After examining the accuracy of the simulation method used, the results of FEA are presented in this section. For this purpose, first, the variable parameters are introduced, and then the outputs of the FEA of the models are shown for each of the states. Finally, the effect of each of the variable parameters on the behavior of the beams is evaluated. As observed in the laboratory strengthening section, variables such as the type of jacket (RC jacket, SPFCJ, CFRP) and the amount of SFs used in the jacket

**TABLE 10.** Percentage difference between laboratory samples and finite element models

Name	Crack load (kN)			Yield load (kN)			Maximum load (kN)		
	EXP.	FEM	Variation (%)	EXP.	FEM	Variation (%)	EXP	FEM	Variation (%)
NR	4.1	3.8	7.9	34.2	34.9	2	52	47.9	8.6
J-F1	9.3	9.6	3.1	68.9	72.6	5.1	93	87.8	5.9
CJ-F1	12.9	13.1	1.5	101	99	2	119	121	1.7
CFRP	5.1	5.4	5.6	62.3	68.4	8.9	90.8	92.6	1.9

(0, 1, and 2% by volume of concrete). Variable parameters in FEA include the strength class of concrete used in the main beam (C15, C20, and C25), the length of the beams (1.4 and 2.8 m), the type of jacket (RC jacket, SPFCJ, CFRP), and jacket thickness (40, 60 and 80 mm). The main beam's compressive strength is considered as a variable because in many RC buildings, the compressive strength of the concrete is not following the designer's purpose (compressive strength characteristic of concrete during design) is significantly different. Therefore, according to the tests provided by reputable concrete laboratories, three common concrete grades in the finite element section were considered for beams. The efficiency of the strengthening method in beams with different compressive strengths can be measured. Also, beam span length was evaluated as one

of the variables in FEA. For this purpose, the span length was doubled so that the performance of the proposed reinforcement methods in longer beams could be evaluated. The thickness of the proposed concrete jackets is also one of the parameters that can affect the results. For this purpose, three thicknesses of 40, 60, and 80 mm were considered for the cover. Thus, at first, the thickness of the jackets was considered to be 40 mm for the initial 24 cases, and then the optimal condition was selected, and the thickness of the jacket was increased by 1.5 and 2 times. The thickness of the steel sheet used in SPFCJs, the thickness of CFRP sheets, the geometrical and mechanical characteristics of longitudinal and transverse steel beams of the main beams, the geometrical and mechanical characteristics of the veneer rebar network, the geometric cross-section of the main beams and the

abutment conditions are fixed in all cases. Table 11 introduces the desired parameters. In this table, the letter C indicates the category of concrete used, and the number after it shows the concrete strength of the main beam in megapascals. The letter L also shows the length of the beam span, and the number after it indicates the length of the beam in megapascals. Also, each of the terms CJ, J, and FRP refer to reinforced beams with concrete-steel composite jackets, concrete jackets, and FRP. Figure 17 presents the geometric characteristics of the beams under study in the finite element study.

**TABLE 11.** Introduces the studied parameters in FEA

No.	Name	Main beam concrete category (MPa)	Beam span (mm)	Jacket thickness (mm)	Jacket type
1	C15-L1.4	15			
2	C20-L1.4	20	1400		
3	C25-L1.4	25			
4	C15-L2.8	15			----
5	C20-L2.8	20	2800		
6	C25-L2.8	25			
7	C15-L1.4-CJ	15			
8	C20-L1.4-CJ	20	1400		
9	C25-L1.4-CJ	25			
10	C15-L2.8-CJ	15			SPFCJ
11	C20-L2.8-CJ	20	2800		
12	C25-L2.8-CJ	25			
13	C15-L1.4-J	15			
14	C20-L1.4-J	20	1400	40	
15	C25-L1.4-J	25			
16	C15-L2.8-J	15			RC Jacket
17	C20-L2.8-J	20	2800		
18	C25-L2.8-J	25			
19	C15-L1.4-CFRP	15			
20	C20-L1.4-CFRP	20	1400		
21	C25-L1.4-CFRP	25			
22	C15-L2.8-CFRP	15			FRP
23	C20-L2.8-CFRP	20	2800		
24	C25-L2.8-CFRP	25			
25	Optimal mode with 60 mm jacket thickness				
26	Optimal mode with 80 mm jacket thickness				

The load was applied in four points similar to the laboratory conditions, and the displacement corresponding to the middle of the span was measured. Figure 18 illustrates how the load is applied to the beams. The details of the beam were presented in the literature [20].

The results of the FEA of beams are presented in four different groups (Figures 19-22). In the first group, outputs related to control beams (without strengthening), in the second group, outputs related to beams strengthened with RC jackets, in the third group, outputs related to beams strengthened with SPFCJ, the fourth group, outputs related to beams strengthened with CFRP sheets are presented. Figure 8 provides a hypothetical load-displacement diagram to introduce the points corresponding to crack, yield, and the maximum bearing load of the beam.

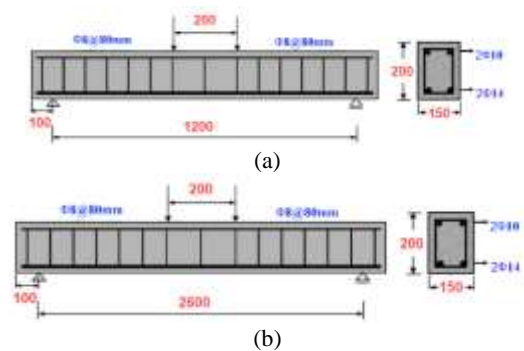


**Figure 17.** Geometric characteristics of finite element model of concrete beams under study (a) 1.4-meter beam (b) 2.8-meter beam

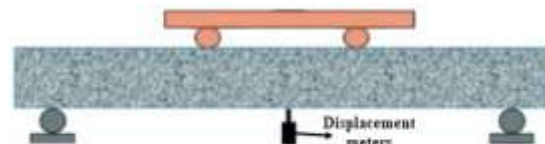


**Figure 18.** Loading

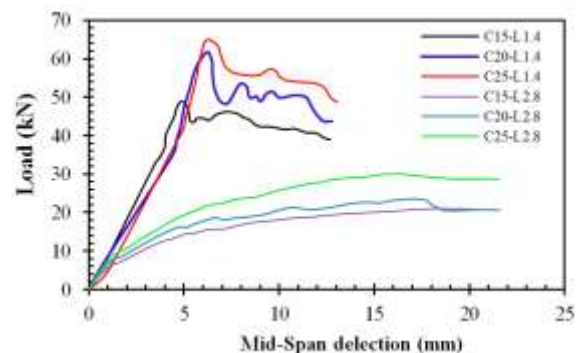


**Figure 19.** Load-mid span deflection curves of control beams (without reinforcement)

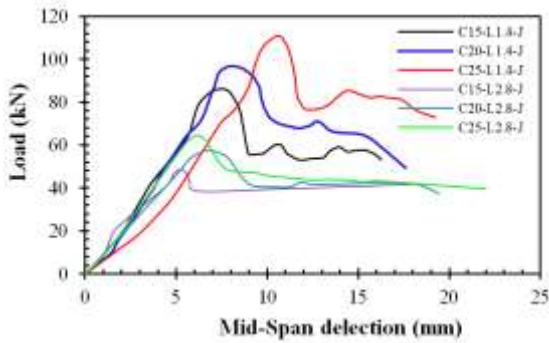


Figure 20. Load-mid span deflection curves of strengthened beams with SPFCJ

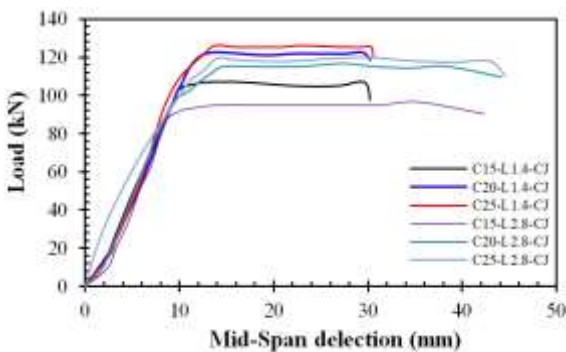


Figure 21. Load-mid span deflection curves of strengthened beams with RC jacket

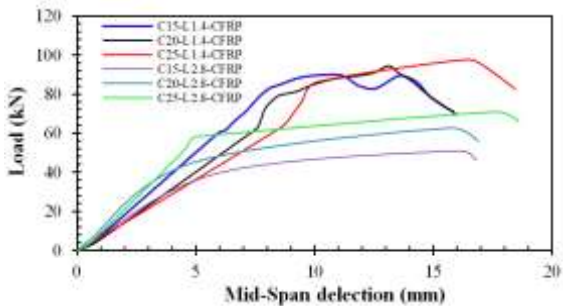


Figure 22. Load-mid span deflection curves of strengthened beams with CFRP sheets

**7. 1. Energy Absorption Capacity**

In Figures 23 and 24, the energy absorption capacity of beams with a span length of 1.40 m and 2.8 m are compared with each other. The addition of SPFCJ containing SFs to the beams is effective for all three categories of concrete used. It has increased the energy absorption capacity by 5.83, 5.83, and 5.63 times, respectively. Also, the addition of RC jackets with SFs to the beams is effective for all three categories of concrete used. It has increased the energy absorption capacity by 1.87, 2.7, and 2.25 times, respectively. The performance of CFRP sheets was almost similar to that of RC jackets. The addition of

CFRP sheets of C15, C20, and C25 beams increased the energy absorption capacity by 2.19, 1.87, and 2.12 times compared to the control sample, respectively.

In Figures 25 and 26, the energy absorption capacity of beams with a span length of 1.4 m and 2.80 m are compared with each other. The addition of SPFCJ to beams with a span length of 2.8 m is effective for all three categories of concrete used. It has increased the energy absorption capacity by 9.72, 11.03, and 9.16 times, respectively. Also, the addition of RC jackets with SFs to the beams is effective for all three categories of concrete used. It has increased the energy absorption capacity by 1.82, 1.91, and 1.8 times, respectively. The addition of CFRP sheets of C15, C20, and C25 grade beams increased the energy absorption capacity by 1.71, 1.93, and 2.02 times compared to the control sample, respectively.

Strength classes of C20 and C25 are classes that are used in many common construction projects, and class C15 is a class that represents the strength of a weak beam. According to Figures 23 to 26, it can be stated that in all three strengthened methods used, the change in the concrete category of the main beam did not significantly change the performance of the methods.

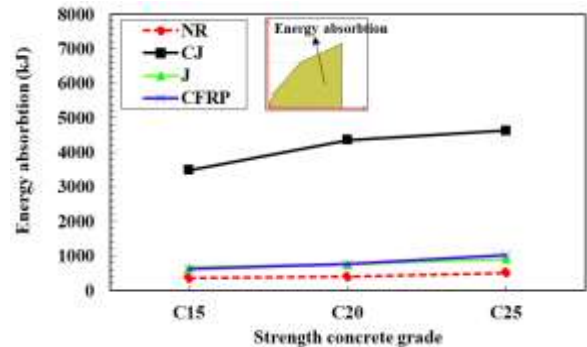


Figure 23. Comparison of energy absorption capacity of beams with a span length of 1.4 m

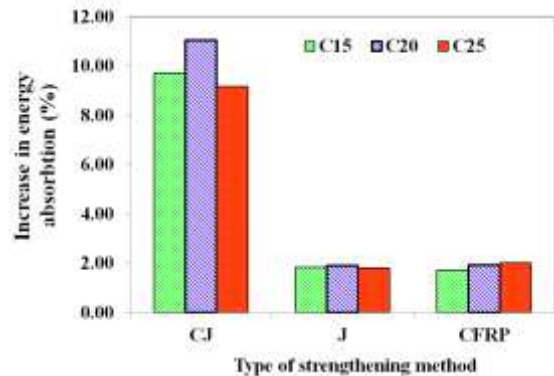
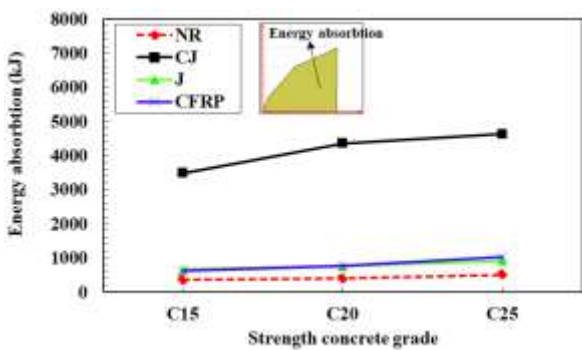


Figure 24. Increase in energy absorption capacity of RC beams compared to non-strengthened beams (control) with a span length of 1.4 m

**TABLE 12.** FEA results

Name	Load			Deflection			Energy absorption (kJ)	Ductility ( $\mu$ )
	Crack (kN)	Yield (kN)	Max. (kN)	Crack (kN)	Yield (kN)	Max. (kN)		
C15-L1.4	3.9	33.4	48	0.5	4.8	12.5	450	2.6
C20-L1.4	4.5	35.6	61	0.6	4.9	12.9	499	2.63
C25-L1.4	4.9	39.1	65	1.4	5.8	13	540	2.24
C15-L2.8	3.4	17	24	1.5	8	21.5	358	2.68
C20-L2.8	3.8	18	26	1.6	8.5	21.3	395	2.5
C25-L2.8	4.1	24	30	1.7	10	21.5	505	2.15
C15-L1.4-CJ	8.5	98	116	2.5	9.1	30.3	2624	3.33
C20-L1.4-CJ	10.8	104	121	2.7	9.6	31.6	2909	3.29
C25-L1.4-CJ	11.1	110	127	2.9	10	32.6	3041	3.26
C15-L2.8-CJ	8.1	86	97	2.2	8.9	42.3	3480	4.75
C20-L2.8-CJ	8.9	91	114	2.3	9.1	44.5	4357	4.89
C25-L2.8-CJ	10.3	96	119	2.4	9.6	45.8	4624	4.77
C15-L1.4-J	8.9	67.5	88	1.1	5.9	16.3	848	2.36
C20-L1.4-J	9.1	69.3	95	1.4	6.25	17.5	1032	2.41
C25-L1.4-J	10.3	70.6	110	1.6	7	19	1214	2.38
C15-L2.8-J	7.9	40.6	48	0.8	4.5	18	653	2.95
C20-L2.8-J	8.3	45.9	55	0.9	5	19	754	3.02
C25-L2.8-J	8.9	58.3	63	1	5.3	22	910	3.28
C15-L1.4-FRP	4	59	88	0.7	6	15	987	2.50
C20-L1.4-FRP	5	61	99.3	0.8	7	16	932	2.29
C25-L1.4-FRP	6.3	63.3	95	0.9	8.5	18.5	1143	2.18
C15-L2.8-FRP	3.5	39	51	0.5	5.9	16.3	612	2.76
C20-L2.8-FRP	4.5	45	63	0.5	4.9	16.9	763	3.45
C25-L2.8-FRP	4.9	51	71	0.6	4.9	18.9	1018	3.86



**Figure 25.** Comparison of energy absorption capacity of beams with span length of 2.8 m

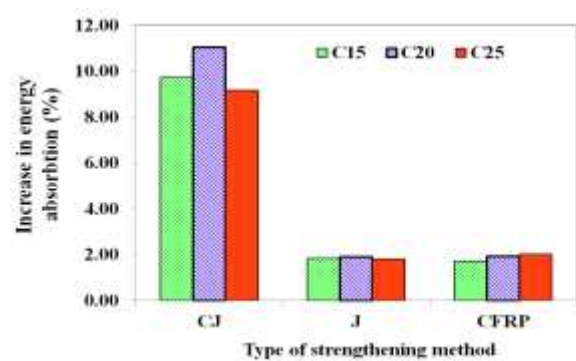


**Figure 26.** Values of percentage increase in energy absorption capacity of RC beams compared to non-reinforced beams (control) with a span length of 2.8 meters

Figure 27 compares the values of percentage increase in energy absorption capacity of RC beams compared to control beams. According to this diagram, the proposed

method has been more effective in longer beams; the SPFCJ in beams with a span length of 2.8 meters has

increased the energy absorption capacity depending on the strength class of the main beam from 9 to 11 times. However, in beams with a span length of 1.4 m, the use of the proposed composite jackets has increased the energy absorption capacity by about 5 to 6 times.

The performance of RC jackets containing SFs and the CFRP method on increasing the bearing capacity of beams for both considered span lengths are almost similar. Depending on the length of the spans and the concrete category of the main beam, the energy absorption capacity is in between 1.8 to 2.5 times.

**7. 2. Comparison of Crack Load Values** The crack load in the studied beams is presented in Figure 28. SPFCJ in all cases has increased the crack resistance of the beams. The crack load of the strengthened beams with the proposed jackets has increased by 2.2 to 2.5 times depending on the strength class of the main beam and the span length. The CFRP method had less effect on increasing the crack load than the other two methods such that using this method, the load on the beams increased by only about 10 to 20%.

**7. 3. Comparison of Yield Load** The point of the load-displacement curve at which the curve fails locally is considered as the yield point. Accordingly, the yield load of the 24 finite element models simulated is presented in Figure 28. The addition of SPFCJ jackets containing SFs increased the yield load of beams with strength classes C15, C20, and C25 and a span of 1.4 m by 2.9, 2.9, and 2.8 times, respectively. The SPFCJ increased the yield load of beams with strength classes C15, C20, and C25 and with a span of 2.8 meters by 1.5, 1.5, and 4 times, respectively.

The effectiveness of reinforced concrete jacket methods containing SFs and CFRP sheets had less effect on improving the yield load of beams compared to the proposed method. The use of concrete jackets containing SFs increased the yield load of beams with resistance classes C15, C20, and C25 and with a span of 1.4 meters by 2, 1.9, and 1.8 times, respectively. The RC jackets

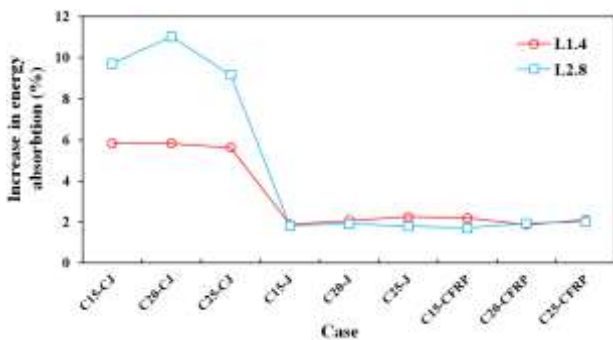


**Figure 27.** Comparison of the energy absorption capacity increase compared to non-strengthened beams (control) to investigate the effect of change along the span

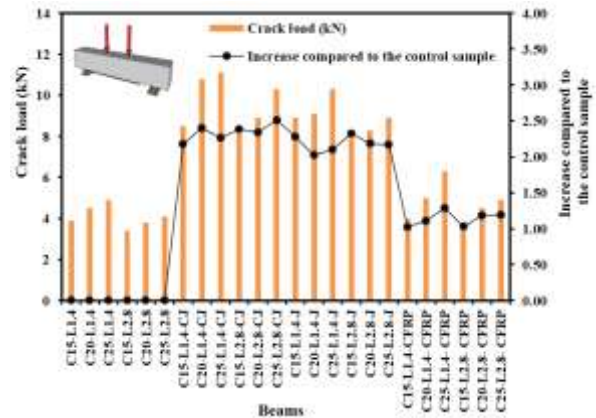


**Figure 28.** Load values corresponding to the first crack in the beams and their increase ratios compared to the control samples

containing SFs increased the yield load of beams with resistance classes C15, C20, and C25 and with a span of 2.8 meters by 2.4, 2.6, and 2.4 times, respectively.

**7. 4. Comparison of Bearing Capacity of Beams (Maximum Load)**

The maximum load that the beam can withstand is called the bearing capacity or maximum load. The load capacity of beams with a span length of 1.4 m, which strengthened using SPFCJ, in which concrete with grades C15, C20, and C25 have been used, increased by 2.4, 2, and 2 times, respectively. Bearing capacity of beams with a span length of 2.8 m, which have been strengthened using SPFCJ in which concrete with grades C15, C20, and C25 have been used, increased by 4, 4.4, and 4 times, respectively (Figure 30). From these values, it can be concluded that the proposed method has a good performance for the three strength classes. Also, the effectiveness of SPFCJ is more effective in beams with longer span lengths.

RC jackets containing SFs increased the maximum load of beams with strength classes C15, C20, and C25 and with a span of 1.4 meters by 1.8, 1.6, and 1.7 times,

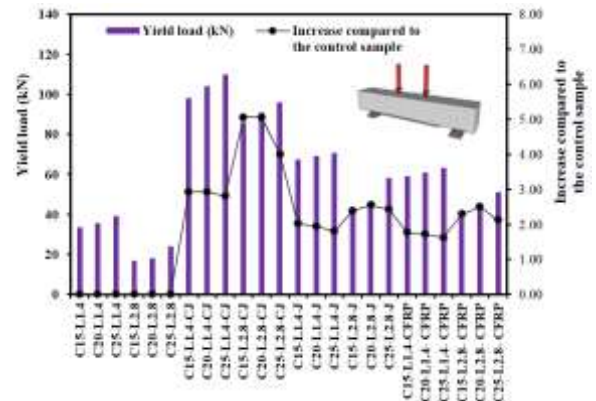


**Figure 29.** The yield values of the beams and their increase ratios in comparison with the control samples

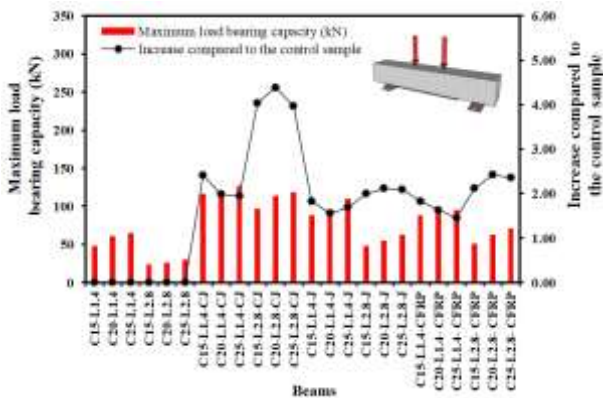


**Figure 30.** Maximum beam load values and their increase ratios compared to control specimens

respectively. RC jackets containing SFs caused the maximum load of beams with strength class C15, C20, and C25 and with a span of 2.8 meters to increase by 2, 1.2, and 1.2 times, respectively. The use of CFRP sheets increased the maximum load of beams with strength classes C15, C20, and C25 and with a span of 1.4 meters by 1.8, 1.6, and 1.5 times, respectively. The use of CFRP sheets increased the maximum load of beams with strength classes C15, C20, and C25 and with a span of 2.8 meters by 2.1, 2.1, and 2.4 times, respectively.

**7. 5. Ductility** Figure 31 compares the ductility coefficient of the studied beams. SPFCJ has increased the ductility of the specimens. SPFCJ makes the beams to withstand larger forces with more ductility. These jackets perform better than concrete fibers strengthened with SFs and CFRP sheets. The ductility of strengthened beams with SPFCJ increases by 22 to 96%, depending on the category of concrete used and span length.

**7. 6. Investigation of the Effect of Change in the Thickness of the Proposed Concrete Jackets**

The thickness of the proposed jackets containing SFs is one of the parameters whose amount can affect the response of the beam. This section examines this parameter. The C25-L1.4-CJ beam performed better than

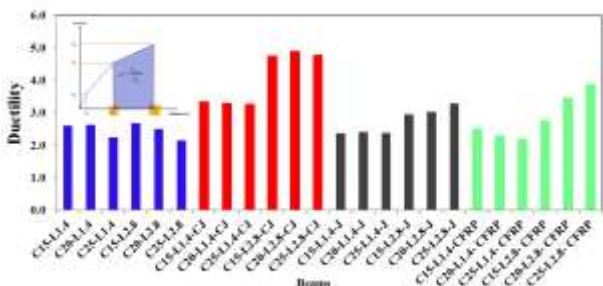


**Figure 31.** Comparison of ductility coefficients of beams in different states

other modes of energy absorption capacity, bearing capacity, crack and yield loads and ductility. The thickness of the cover of this beam was 40 mm. The mentioned beam was simulated again with two different jacket thicknesses (60 and 80 mm), and the results of its analysis were presented in Figures 32 and 33.

In the beam that was strengthened using the C25-L1.4-CJ-t60 jacket, the crack, yield, and maximum beam loads were 46, 196, and 228 kN, respectively. Also, the corresponding displacements with crack and yield loads were equal to 0.3 and 6.47 mm, respectively. The ultimate displacement of this beam was 32 mm.

According to Figure 33 in the beam that was strengthened using the C25-L1.4-CJ-t80 jacket, the crack loads, yield, and maximum loads were 32, 147, and 190 kN, respectively. Also, the corresponding displacements to crack and yield loads were equal to 0.49 and 5.8 mm, respectively.

Figure 34 and Table 13 compare the load-deflection curves of strengthened beams with SPFCJ to investigate changes in the thickness of the jacket. Among the three thicknesses considered for jackets, 60 mm thick has the best performance in terms of energy absorption capacity compared to the other two thicknesses. Energy absorption capacity corresponding to the C25-L1.4-CJ-t60 mode is approximately two times that of the C25-L1.4-CJ-t40 mode and 18% higher than the C25-L1.4-CJ-t80 mode. In terms of load-bearing capacity or maximum load-bearing capacity, jackets with a thickness of 60 mm had a relatively better performance; So that the bearing capacity of the strengthened beam with 60 mm composite jacket has been increased by 79 and 20% more than the values corresponding to 40 and 80 mm jackets.

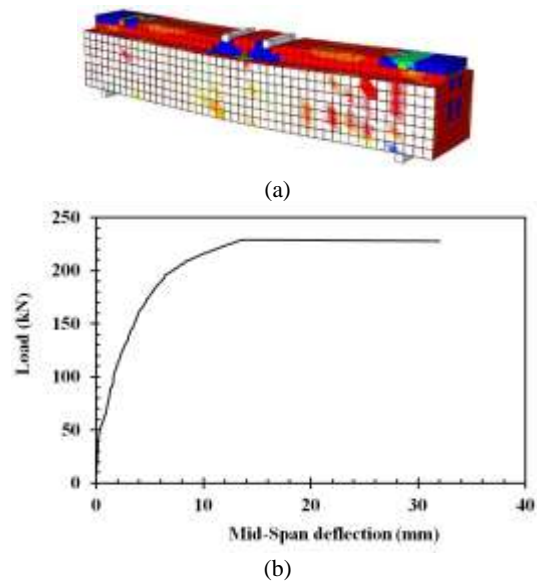


**Figure 32.** Results of analysis of C25-L1.4-CJ beam with 60 mm jacket thickness a: Crack distribution and deformable shape b: Load-deflection curve

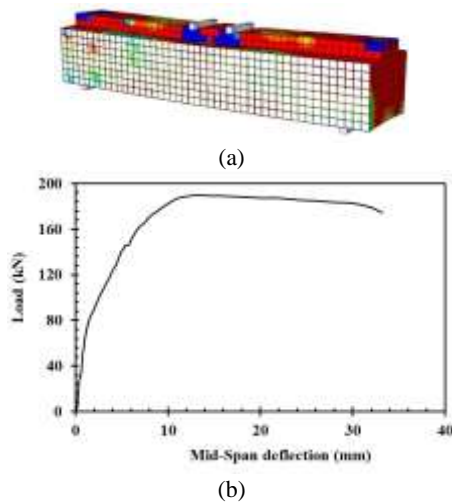


**Figure 33.** Results of C25-L1.4-CJ beam analysis with 80 mm jacket thickness (a) Crack distribution and modified shape (b) load-displacement curve

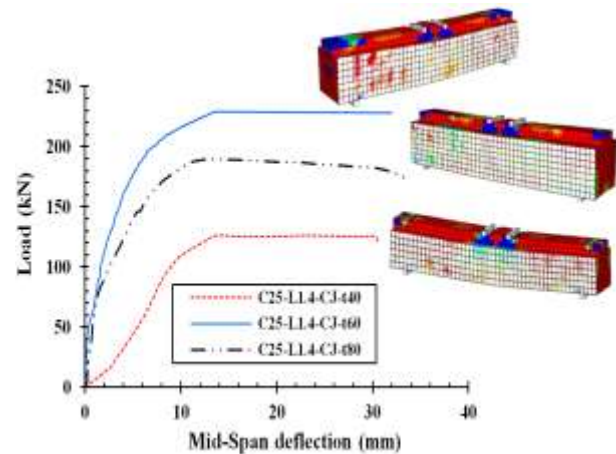


**Figure 34.** Comparison of load-deflection curves of strengthened beams with SPFCJ to investigate changes in jacket thickness

**TABLE 13.** Comparison of strengthened beams to investigate the effect of change in the thickness of the proposed composite jacket

Name	Load (kN)			Deflection (mm)			Ductility	Energy absorption (J)
	Crack	Yield	Max.	Crack	Yield	Max.		
C25-L1.4-CJ-t40	11.1	110	127	2.9	10	32.6	3.26	3041
C25-L1.4-CJ-t60	46	196	228	0.3	6.47	32	4.94	6597
C25-L1.4-CJ-t80	32	147	190	0.49	5.8	33.9	5.84	5585

It can be said that the jacket thickness parameter has a significant role in the response of strengthened beams with the proposed composite jackets, and depending on the dimensions and geometric characteristics of the beam, a suitable thickness should be considered for the jacket.

## 8. CONCLUSIONS

In this study, the strengthening of RC beams using SPFCJ jackets was investigated. For this purpose, the effect of parameters such as compressive strength of the main concrete beam jacket thickness and span length using FEA, was evaluated. The accuracy of the FEA method was evaluated by modeling a number of laboratory beams prepared by Shadmand et al. [20], and it was shown that the method used can provide an accurate prediction of the beam response. This section summarizes some of the most important results:

- The ductility of strengthened beams with SPFCJ jackets containing SFs has increased from 26 to 52%, depending on the amount of fibers compared to the control sample. As the concrete jacket contains fibers, the beams can withstand more forces with more ductility.

- Strength classes C20 and C25 are classes that are used in many common construction projects, and class C15 is a class that represents the resistance of a weak beam. In all three reinforcement methods used, the change in the concrete category of the main beam did not significantly change the performance of the proposed method.
- The proposed method has been more effective in longer beams. The SPFCJ in beams with a span length of 2.8 meters has increased the energy absorption capacity depending on the strength class of the main beam from 9 to 11 times. In beams with a span length of 1.4 m, the proposed composite jackets have increased the energy absorption capacity by about 5 to 6 times.
- SPFCJ in all cases has increased the crack resistance of the beams; So that the crack load of the reinforced beams with the proposed jackets has increased 2.2 to 2.5 times depending on the resistance class of the main beam and the span length. The CFRP method had less effect on increasing the crack load than the other two methods. Using this method, the load on the beams increased by only about 10 to 20%.
- The bearing capacity of beams with a span length of 2.8 m, which have been strengthened using SPFCJ with grades C15, C20, and C25, increased 4, 4.4, and

4 times, respectively. From these values, it can be concluded that the proposed method has a good performance for the three strength. Also, the effectiveness of SPFCJ is more effective in beams with longer span lengths.

The strengthened beams with SPFCJ can depend on several factors. Therefore, to develop the present study, the following suggestions are presented:

- Investigating the effect of changing the percentage of steel reinforcement used in the main beams on the present study results.
- Investigating the use of other fibers such as basalt and polypropylene in RC jackets to strengthen concrete beams.
- Combined use of nanoparticles and types of fibers such as basalt, glass, and polypropylene in RC jackets to strengthen these beams.
- Investigation of strengthening of RC beams with composite jackets strengthened with SFs against cyclic loading.

## 9. REFERENCES

1. Khan, MA., "Toward Key Research Gaps in Design Recommendations on Flexurally Plated RC Beams Susceptible to Premature Failures." *Journal of Bridge Engineering*, Vol. 26, No. 9, (2021), 04021067. Doi: doi.org/10.1061/(ASCE)BE.1943-5592.0001772
2. Deng, Y., Ma, F., Zhang, H., Wong, S. H., Pankaj, P., Zhu, L., & Bahadori-Jahromi, A., "Experimental study on shear performance of RC beams strengthened with NSM CFRP prestressed concrete prisms." *Engineering Structures*, Vol. 235, (2021), 112004. Doi: doi.org/10.1016/j.engstruct.2021.112004
3. Yuan, P., Xiao, L., Wang, X., & Xu, G., "Failure mechanism of corroded RC beams strengthened at shear and bending positions." *Engineering Structures*, Vol. 240, (2021), 112382. Doi: doi.org/10.1016/j.engstruct.2021.112382
4. Liu, X., Gernay, T., Li, L. Z., & Lu, ZD., "Seismic performance of post-fire reinforced concrete beam-column joints strengthened with steel haunch system." *Engineering Structures*, Vol. 234, (2021), 111978. Doi: doi.org/10.1016/j.engstruct.2021.111978
5. Ozturk, B., Yilmaz, C., Şentürk, T. "Effect of FRP retrofitting application on seismic behavior of a historical building at Nigde, Turkey", 14th European Conference on Earthquake Engineering. (2010), Ohrid, Republic of Macedonia.
6. Ozturk, B. A. K. İ., Sentürk, T., Yilmaz, C. "Analytical investigation of effect of retrofit application using CFRP on seismic behavior of a monumental building at historical Cappadocia region of Turkey", (2010), In 9th US National and 10th Canadian Conference on Earthquake Engineering, Toronto, Canada.
7. Shen, D., Li, M., Kang, J., Liu, C., Li, C., "Experimental studies on the seismic behavior of reinforced concrete beam-column joints strengthened with basalt fiber-reinforced polymer sheets." *Construction and Building Materials*, Vol. 287, (2021), 122901. Doi: doi.org/10.1016/j.conbuildmat.2021.122901
8. Nie, XF., Zhang, SS., Yu, T., "On the FE modelling of RC beams with a fibre-reinforced polymer (FRP)-strengthened web opening." *Composite Structures*, Vol. 271, (2021), 114161. Doi: doi.org/10.1016/j.compstruct.2021.114161
9. Rahmani, I., Maleki, A., Lotfollahi-Yaghin, MA., "A laboratory study on the flexural and shear behavior of rc beams retrofitted with steel fiber-reinforced self-compacting concrete jacket". *Iranian Journal of Science and Technology*, (2020), 1-17. Doi: doi.org/10.1007/s40996-020-00547-x
10. Maraq, MA., Tayeh, BA., Ziara, MM., Alyousef, R., "Flexural behavior of RC beams strengthened with steel wire mesh and self-compacting concrete jacketing—experimental investigation and test results." *Journal of Materials Research and Technology*, Vol. 10, (2021), 1002-1019. Doi: doi.org/10.1016/j.jmrt.2020.12.069
11. Faez, A., Sayari, A., & Manei, S., "Retrofitting of RC beams using reinforced self-compacting concrete jackets containing aluminum oxide nanoparticles." *International Journal of Engineering, Transactions B: Applications*, Vol. 34, No. 5, (2021), 1195-1212. Doi: 10.5829/ije.2021.34.05b.13
12. Mohsenzadeh, S., Maleki, A., Lotfollahi-Yaghin, MA., "Strengthening of RC beams using SCC jacket consisting of glass fiber and fiber-silica fume composite gel". *International Journal of Engineering, Transactions B: Applications*, Vol. 34, No. 8, (2021), 1923-1939. Doi: 10.5829/ije.2021.34.08b.14
13. Attar, H. S., Esfahani, M. R., Ramezani, A. "Experimental investigation of flexural and shear strengthening of RC beams using fiber-reinforced self-consolidating concrete jackets." *In Structures*, Vol. 27, (2020), 46-53. Doi: doi.org/10.1016/j.istruc.2020.05.032
14. Kim, MS., Lee, YH., "Flexural Behavior of Reinforced Concrete Beams Retrofitted with Modularized Steel Plates" *Applied Sciences*, Vol. 11, No. 5, (2021), 2348. Doi: doi.org/10.3390/app11052348
15. Rahimi, SB., Jalali, A., Mirhoseini, SM, Zeighami, E., "Experimental Comparison of Different Types of FRP Wrapping in Repairing of RC Deep Beams with Circular Openings". *International Journal of Engineering, Transactions B: Applications*, Vol. 34, No. 8, (2021), 1961-1973. doi: 10.5829/ije.2021.34.08b.17
16. Artiningsih, T. P., Lirawati, L., Helmi, N., "Retrofitting of Reinforced Concrete Beams Using a Fiberglass Jacketing System." *Journal of Advanced Civil and Environmental Engineering*, Vol. 4, No. 1, (2021), 44-50. Doi: doi.org/10.30659/jacee.4.1.44-50
17. Do Thi, MD., Lam, TQK., "Design parameters of steel fiber concrete beams." *Magazine of Civil Engineering*, Vol. 2, (2021), 10207-10207. Doi: 10.1007/978-981-33-6208-6\_30
18. Kang, MC., Yoo, DY., Gupta, R., "Machine learning-based prediction for compressive and flexural strengths of steel fiber-reinforced concrete." *Construction and Building Materials*, Vol. 266, (2021), 121117. Doi: doi.org/10.1016/j.conbuildmat.2020.121117
19. Awolusi, TF., Oke, OL., Atoyebi, OD., Akinkulore, O., Sojobi, AO., "Waste tires steel fiber in concrete: A review." *Innovative Infrastructure Solutions*, Vol. 6, Vol. 1, (2021), 1-12. Doi: doi.org/10.1007/s41062-020-00393-w
20. Shadmand, M., Hedayatnasab, A., Kohnehpooshi, O., "Retrofitting of reinforced concrete beams with steel fiber reinforced composite jackets". *International Journal of Engineering, Transactions B: Applications*, Vol. 33, No. 5, (2020), 770-783. Doi: 10.5829/ije.2020.33.05b.08
21. Hibbitt, H., Karlsson, B., and Sorensen, E., "ABAQUS user's manual." Providence, RI: Dassault Systems Simulia Corp, (2016).
22. ASTM C143 / C143M-20, Standard Test Method for Slump of Hydraulic-Cement Concrete, ASTM International, West Conshohocken, PA, (2020).

23. ASTM Standard C39/C39M-18, Standard test method for compressive strength of cylindrical concrete specimens, ASTM International, West Conshohocken PA, (2018).
24. ASTM C293/ C293M-16, Standard Test Method for Flexural Strength of Concrete (Using Simple Beam With Center-Point Loading), ASTM International, West Conshohocken, PA, (2016).
25. ASTM Standard C496/C496M-17 Standard test method for splitting tensile strength of cylindrical concrete specimens, ASTM International, West Conshohocken PA, (2017).
26. Standard practice for selecting proportions for normal, heavyweight, and mass concrete, ACI 211.1-91 (1991), ACI Committee 211, Farmington Hills, MI, USA.
27. Soon, Poh Yap., Kuan Ren Khaw, U., Johnson Alengaram, Mohd Zamin Jumaat., "Effect of fiber aspect ratio on the torsional behavior of steel fiber-reinforced normal weight concrete and lightweight concrete." *Engineering Structures* Vol. 101, (2015), 24– 33. Doi: 10.1016/j.engstruct.2015.07.007
28. Han, J., Zhao, M., Chen, J., Lan, X. "Effects of steel fiber length and coarse aggregate maximum size on mechanical properties of steel fiber reinforced concrete." *Construction and Building Materials*, Vol. 209, (2019), 577-591. Doi: 10.1016/j.conbuildmat.2019.03.086
29. Wu, Z., Shi, C., He, W., Wu, L., "Effects of steel fiber content and shape on mechanical properties of ultra high performance concrete." *Construction and Building Materials*, Vol. 103, (2016), 8-14. Doi: doi.org/10.1016/j.conbuildmat.2015.11.028
30. Song, PS., Hwang, S., "Mechanical properties of high-strength steel fiber-reinforced concrete," *Construction and Building Materials* Vol. 18 (2004). Doi: doi.org/10.1016/j.conbuildmat.2004.04.027
31. Abbass, W., Khan, MI., Mourad, S., "Evaluation of mechanical properties of steel fiber reinforced concrete with different strengths of concrete." *Construction and Building Materials*, Vol. 168, (2018), 556-569. Doi: doi.org/10.1016/j.conbuildmat.2018.02.164
32. Madandoust, R., Ranjbar, MM., Ghavidel, R., Shahabi, SF., "Assessment of factors influencing mechanical properties of steel fiber reinforced self-compacting concrete." *Materials & Design*, Vol. 83, (2015), 284-294. Doi: 10.1016/j.matdes.2015.06.024
33. Neves, Rui D., J. C. O, Fernandes de Almeida., "Compressive behaviour of steel fibre reinforced concrete." *Structural Concrete*, Vol. 6, No.1, (2005), 1-8.
34. Cardoso, DC., Pereira, GB., Silva, FA., Silva Filho, JJ., Pereira, EV., "Influence of SFs on the Flexural Behavior of RC Beams with Low Reinforcing Ratios: Analytical and Experimental Investigation" *Composite Structures*, (2019). 110926. Doi: doi.org/10.1016/j.compstruct.2019.110926
35. Ying, H., Huawei, P., Xueyou, Q., Jun, P., Xiancun, L., Qiyun, P., Bao, L., "Performance of Reinforced Concrete Beams Retrofitted by a Direct-Shear Anchorage Retrofitting System." *Procedia Engineering*, Vol. 210, (2017), 132-140.
36. Abdulla, Jabr., "Flexural Strengthening of RC beams using Fiber Reinforced Cementitious Matrix." FRCM, University of Windsor Scholarship at UWindsor, (2017). Doi: 10.1061/(ASCE)CC.1943-5614.0000473
37. Abdallah, M., Al Mahmoud, F., Boissiere, R., Khelil, A., Mercier, J., "Experimental study on strengthening of RC beams with Side Near Surface Mounted technique-CFRP bars." *Composite Structures*, Vol. 234, (2020), 111716. Doi: doi.org/10.1016/j.compstruct.2019.111716
38. Nanda, RP., Behera, B., "Experimental study of shear-deficient RC beam wrapped with GFRP." *International Journal of Civil Engineering*, Vol. 18, No. 6, (2020), 655-664. Doi: doi.org/10.1007/s40999-020-00498-4
39. Yu, F., Zhou, H., Jiang, N., Fang, Y., Song, J., Feng, C., Guan, Y., "Flexural experiment and capacity investigation of CFRP repaired RC beams under heavy pre-damaged level." *Construction and Building Materials*, Vol. 230, (2020) 117030. Doi: 10.1016/j.conbuildmat.2019.117030
40. Zhang, Y., Li, X., Zhu, Y., Shao, X., "Experimental study on flexural behavior of damaged reinforced concrete (RC) beam strengthened by toughness-improved ultra-high performance concrete (UHPC) layer." *Composites Part B: Engineering*, Vol. 186, (2020), 107834. Doi: doi.org/10.1016/j.compositesb.2020.107834
41. Lubliner, J., Oliver, J., Oller, S., Onate, E. "A plastic-damage model for concrete" *International Journal of Solids and Structures*, Vol. 25, No. 3, (1989), 299-326.
42. Shoja, E., Alielahi, H. (2020). An Investigation of the Seismic Interaction of Surface Foundations and Underground Cavities Using Finite Element Method. *International Journal of Engineering, Transactions C: Aspects*, Vol. 33, No. 9, 1721-1730. doi: 10.5829/ije.2020.33.09c.04
43. Bagheripourasil, M., Mohammadi, Y., Gholizad, A. "Progressive Collapse Analysis Methods Due to Blast Loading in Steel Moment Frames." *Journal of Modeling in Engineering*, Vol. 15, No. 51, (2017), 51-65. DOI: 10.22075/jme.2017.2688
44. Kaafi, P., Ghodrati Amiri, G. "Investigation of the Progressive Collapse Potential in Steel Buildings with Composite Floor System." *Journal of Structural Engineering and Geotechniques*, Vol. 10, No. 2, (2020), 1-8.
45. Kmiecik, P., Kamiński, M., "Modelling of reinforced concrete structures and composite structures with concrete strength degradation taken into consideration." *Archives of Civil and Mechanical Engineering*, Vol. 11, No. 3, (2011), 623-636. Doi: doi.org/10.1016/S1644-9665(12)60105-8

## Persian Abstract

## چکیده

در مطالعه حاضر رفتار تیرهای بتنی مسلح مقاوم سازی شده با ژاکت‌های کامپوزیتی فولادی - بتنی مسلح به الیاف فولادی با استفاده از تحلیل اجزاء محدود ارزیابی شده است. همچنین صحت روش تحلیل با مدلسازی تعدادی تیر بتنی مسلح که در آزمایشگاه ساخته شد، ارزیابی گردید و تطابق مناسبی مشاهده گردید. پارامترهای متغیر در تحلیل اجزاء محدود به ترتیب شامل رده مقاومتی بتن مورد استفاده در تیر اصلی (۱۵، ۲۰ و ۲۵ مگاپاسکال)، طول دهانه تیرها (۱.۴ و ۲.۸ متر)، نوع روکش (روکش بتنی مسلح، روکش بتنی مسلح حاوی الیاف فولادی، روکش کامپوزیت فولادی - بتنی حاوی الیاف فولادی، ورق CFRP) و ضخامت روکش (۴۰، ۶۰ و ۸۰ میلیمتر) می‌باشند. دلیل اینکه مقاومت فشاری تیر اصلی به عنوان متغیر در نظر گرفته شده است آن است که در بسیاری از ساختمان‌های بتنی مسلح، مقاومت فشاری بتن مورد نظر مطابق با اهداف طراح (مقاومت فشاری مشخصه بتن در هنگام طراحی) نمی‌باشد و تفاوت قابل توجهی دارد. نتایج تحلیل اجزاء محدود نشان داد که افزودن روکش‌های بتنی مسلح به الیاف فولادی به تیرها برای هر سه رده بتن مصرفی موثر می‌باشد و توانسته ظرفیت جذب انرژی را به ترتیب ۱.۸۸، ۲.۰۷ و ۲.۲۵ برابر افزایش دهد. از بین سه ضخامت در نظر گرفته شده برای روکش‌ها، از جنبه ظرفیت باربری روکش‌های با ضخامت ۶۰ میلیمتر عملکرد نسبتاً بهتری داشتند؛ بطوریکه ظرفیت باربری تیر مقاوم سازی شده با روکش کامپوزیتی ۶۰ میلیمتری به مقدار ۷۹ و ۲۰ درصد بیشتر از مقادیر متناظر با روکش‌های ۴۰ و ۸۰ میلیمتری شده است. پارامتر ضخامت روکش نقش قابل توجهی بر پاسخ تیرهای مقاوم سازی با روکش‌های کامپوزیتی پیشنهادی دارد و بسته به ابعاد و مشخصات هندسی تیر می‌بایست، ضخامت مناسبی را برای روکش در نظر گرفت و افزایش ضخامت همواره نمی‌تواند منجر به بهبود پاسخ تیر شود.